Раздел четвертый

ФИЗИКА РАДИАЦИОННЫХ И ИОННО-ПЛАЗМЕННЫХ ТЕХНОЛОГИЙ

ION BEAM-ASSISTED DEPOSITION TECHNOLOGY AS A METHOD OF NANOCRYSTALLINE COATING FORMATION

Review article

A.G. Guglya, I.G. Marchenko
National Science Center "Kharkov Institute of Physics and Technology", Kharkov, Ukraine
E-mail: guglya@kipt.kharkov.ua

This scientific paper describes the structure, phase composition and mechanical properties of nanocrystalline coatings obtained using the ion beam-assisted deposition technology. The results of computer simulation of IBAD processes for different energy values of bombarding ions and for relationships between the densities of ion fluxes and metal deposition rates is given. The data of electron-microscope analysis of the initial stages of film structure formation (of 5 nm thick and more) is presented. And finally we demonstrate the influence produced by the ion energy and ion current density on the formation of nanocrystalline structure and its correlation with tribological properties of coatings.

PACS: 81.15Jj;81.07Bc;61.20Ja

INTRODUCTION

Perennial attempts made by the researchers in different countries of the world, who work in the field of production and application of thin-films, to develop technologies that would improve the structure-phase stability of such thin films resulted in the development of physical vapor deposition methods (PVD). The success achieved in this field can in many respects be attributed to the creation of different plasma plants and accelerated ion sources in the early sixties. It has been established that an increase in the ion component in the flux of deposited metal atoms and molecules results in a considerable change in the structure and properties of produced films. The use of nitrogen, carbon and boron ions as charged particles allowed for the formation of coatings made of nitrides, carbides and borides whose performance characteristics considerably surpassed those of metals.

An ever-increasing demand for the extension of the resource of articles operating under high mechanical loads, elevated temperatures and corrosion media promoted the development of such coating deposition technologies that allow for the formation of a coating structure by intensive bombardment with ions of > 100 eV. The purpose of ion bombardment is to provide controllable variation of the progress rate of diffusion processes, grain nucleation and growth conditions and also an increase in chemical activity of atoms. To produce such coatings nowadays solely no equilibrium technologies are used that include the stimulation bombardment of a deposited material with gas ions whose energy ranges from several tens of eV to tens of keV (Table). These methods include traditional PVD methods including unbalanced magnetron sputtering (UBM) and ion beam-assisted deposition (IBAD).

Physical phenomena that occur in the depth and on the surface of the material exposed to ion bombardment differ for different technologies. Fig. 1 schematically shows most of those processes.

PVD and UMS methods usually deal with processes that occur on the film surface. As for the IBAD method the depth pass of gas ions reaches 100nm. Therefore their influence on the structure and phase composition is not limited by the film surface region; it captures approximately the same film thickness (Fig. 1). The main processes that take place on the film surface in this connection are as follows: surface diffusion promotion and the creation of surface defects that are the major centers of grain nucleation and also maintenance of the high flow of radiation defects, which provides the formation of stoichiometric Me-(N,O,C) compounds and highly dispersed structure stabilization. While comparing the parameters of technological processes given in Table the attention should be paid to the first two, in particular accelerating potential (ion energy) and working gas pressure in the chamber. It is seen that the IBAD method differs by high ion energy and low gas pressure in the process chamber. High energy provides good coating adhesion due to the ballistic mixing of condensed atoms with substrate atoms. PVD and UMS methods employ high process temperature for the mixing. The IBAD method requires no high temperature maintenance, which allows for the formation of the film structure in no equilibrium conditions. Particularly at such conditions the nucleation and growth of ultrafine grains of 5 to 10 nm (nano grains) take place. It should be noted that in the case of the IBAD method the structure formation is not ended at the nucleation stage. The film material is exposed to the gas ion beam until the thicknesses of ~100 nm is reached; this provides stabilization both of component composition and grain size. The advantage of low pressure inside the process chamber is that the formed coatings have low porosity and low pollution with gas impurities. And finally, in the case of the IBAD technology metal evaporators and gas ion sources are spaced and this provides an opportunity to independently control each parameter of the ion-assisted deposition process and have stable impact on the coating structure. Fig. 2 gives diagrams of two the most spread configurations of the IBAD method.

PVD, UMS and IBAD methods performances

	PVD	UMS	IBAD
E, U_d, (V)	20-300	0-200	500-50000
Gas pressure, Pa	0.05…8.0	0.05…1.0	10^{-2}…10^{-3}
T, ^oC	200…600	100…400	20…200
Working gas	N_2	Ar + N_2	Ar or N_2
Damages, eV/at.	10…10^2	1.0…10	10^2…10^4
Depth of the damaged zone, nm	1…5	<1	10…100

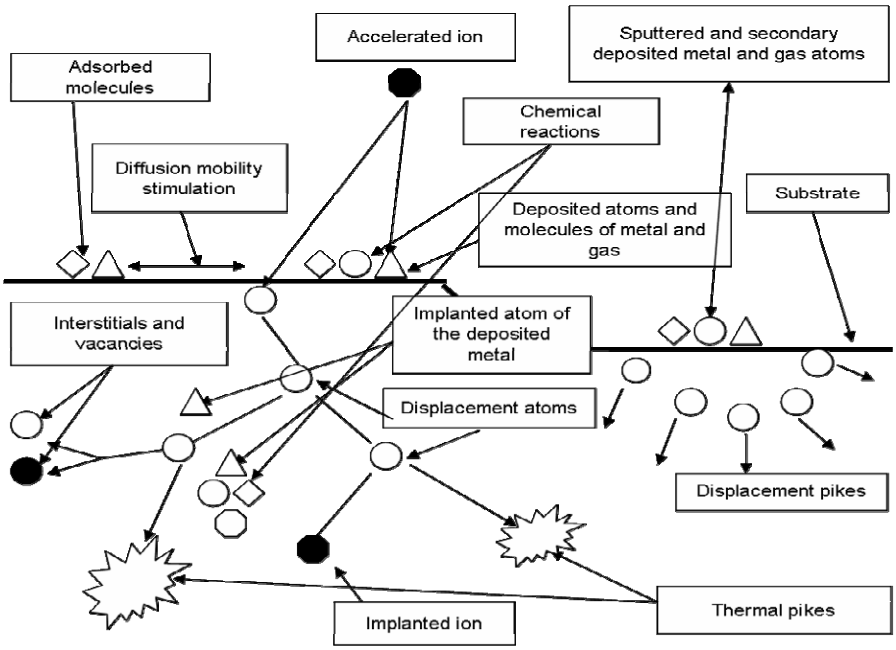

Fig. 1. Surface and in-depth physical phenomena of the IBAD process

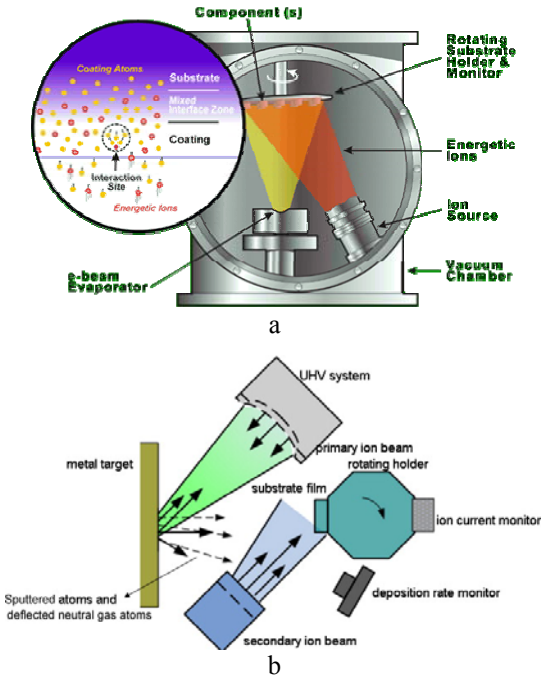

Fig. 2. The main variants of IBAD technology realisation:
a – e-beam metal evaporation + ion bombardment;
b – ion-beam metal sputtering + ion bombardment

The option given in Fig. 2,a has more opportunities for the rate control of metal evaporation and therefore it is employed by industrial ion beam-assisted deposition plants.

1. COMPUTER SIMULATION OF THE ION BEAM-ASSISTED DEPOSITION

To simulate the process of ion beam –assisted deposition we used a computer SRIM program of atom –atom collisions [1]. A peculiar feature of this method is that the portion of ions is reflected from the surface reducing thus total ion flux during the bombardment of deposited film with ions. The interaction of ions with the surface results in the sputtering of deposited film and the rate of its growth is reduced. In the steady-state mode the film boundary moves at a rate V along the "x"-axis. In time t the profile of interstitial atoms $g(x,t)$ shifts together with the boundary of a growing film. During time t the concentration of interstitial atoms at a point x will change by a value of $\Delta c(x) = j_i \int_0^t g(x,t)dt$, where j_i is the flux density of incident ions. We consider the stationary process of film growth and therefore $g(x,t) = g(x - Vt,0)$. It means that the profile of an implanted dopant is simply shifted with time. The concentration at a point x can be found through the integration.

$$C(x) = \frac{j_i}{V} \int_{x-Vt}^{x} g(u)du\,, \qquad (1)$$

On elapse of some time t_{st} the stationary nitrogen distribution $C_{st}(x)$ should be established, which in the future shifts together with the surface. Its value can be derived if characteristics of atomic and ion flows are known.

$$C_{st} = \frac{j_i(1-\gamma)}{V} = \frac{j_i(1-\gamma)}{j_a - j_i S}\rho_s\,, \qquad (2)$$

Where γ is the ion reflection coefficient; S is the integral sputtering ratio; j_i is the ion current density, j_a is the flux density of deposited atoms, ρ_s is the near-surface atomic density of synthesized film material.

In the general case the film growth rate is a function of time and can be derived from the balance between the flow of deposited atoms j_a and sputtered near-surface atoms:

$$V = (j_a + j_i \cdot (1-S))/\rho_s\,, \qquad (3)$$

Fig. 3 shows the dependance of nitrogen concentration in the substrate and deposited chrome film on time during the implantation of ions of 15 and 30 keV at room temperature, when the diffusion mobility of implanted dopant is low [2].

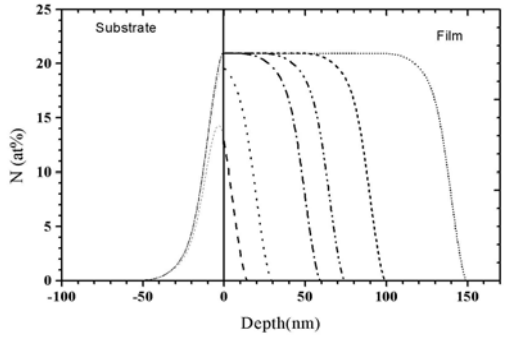

a

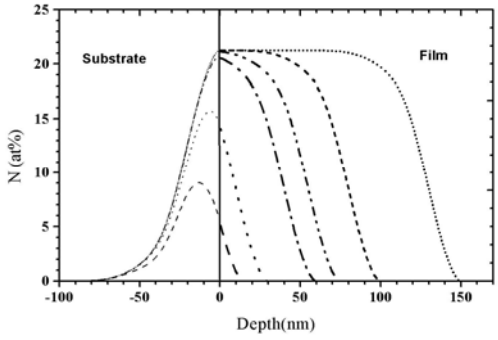

b

Fig. 3. Distribution of nitrogen in the depth of growing Cr film under N_2^+ bombardment. The ion flux – 10^{14} ion/cm^2·s, the film growth rate – 8 nm/min; a – E = 15 keV and b – E = 30 keV. Different curves correspond to the different thickness of the deposited film (- - – 15 nm; · · · – 30 nm; -·-·- – 60 nm; ··-··- – 75 nm; -- – 100 nm; … – 150 nm) [2]

At the beginning of the deposition an abrupt increase in nitrogen concentration in the substrate is observed. Afterwards the dopand concentration reaches a maximum value c_{st}, which corresponds to the steady-state concentration in the depth of deposited film. The distance of nitrogen ion penetration is longer in case of the radiation with ions of 30 keV. Accordingly, the substrate-film mixing zone is also larger.A stationary stage of the IBAD process is also characterised by the availability of the region on the growing film surface whose nitrogen concentration varies from a maximum value to zero. It implies the existance of unformed zone. The higher the ion energy the wider this zone.

The width of mixing zone and that of underformed zome depends not only on the energy of bombarding ions but also on substrate and deposited film materials. Fig. 4 shows the nitrogen distribution at the stationary stage of the IBAD process for the cases of chrome-on-chrome and aluminium-on-aluminium deposition [2]. It is seen that the penetration depth of nitrogen ions into the aluminium substrate exceeds that for the chrome substrate (a mixing zone is larger). At the same time the width of the underformed zone of chrome coating is smaller in comparison with that for alunimium coating.

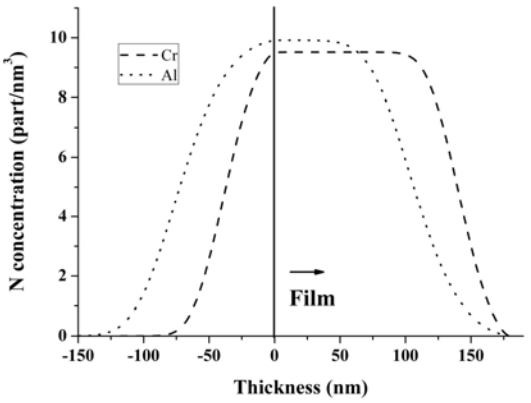

Fig. 4. Sample thickness change of nitrogen concentration during deposition of aluminum and chrome onto substrates made of the same material at simultaneous bombardment with nitrogen ions of 30 keV during 1800 s, $j = 10^{14}$ ion/cm^2/s [2]

To study the processes of a change in chemical composition of the near-surface region during the ion-assisted deposition taking into consideration diffusion processes the following diffusion equation can be used:

$$\frac{\partial C}{\partial t} = \frac{\partial}{\partial x}(D\frac{\partial}{\partial x}C) - V\frac{\partial}{\partial x}C + g(x)\,, \qquad (4)$$

where $C = C(x,t)$ is the nitrogen concentration, D is the diffusion coefficient, $g(x)$ is the concentration of nitrogen imbedded per time unit. The x coordinate is normal to the sample surface. The addend in the left side of equation is defined by the choice of coordinate system, which moves together with the solid body surface.

Fig. 5 shows the sample depth change of the concentration of implanted nitrogen as the diffusion coefficient is increased. Different curves correspond to different nitrogen diffusion coefficients.

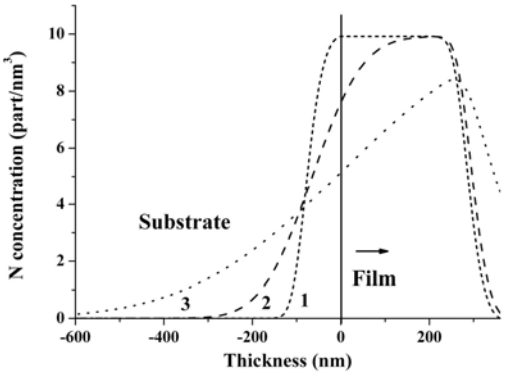

Fig. 5. Sample thickness change in nitrogen concentration during the aluminum deposition onto the substrates made of the same metal at simultaneous bombardment with nitrogen ions of 30keV during 3600 s 1 – 0.01 nm²/s; 2 – 1.0 nm²/s; 3 – 10.0 nm²/s

Figure shows that the mixing zone thickness is increased with an increase in diffusion mobility. The nitrogen concentration at the growing film front is increased due to the migration of implanted nitrogen from the maximum position of occurrence to the film surface. It can also be seen that at high temperatures of the IBAD-process (D-10) the nitrogen concentration in the film depth fails to reach a stationary value during the estimated time (3600 s) of film deposition.

To check the compliance of the results of computer simulation with experimental data using the secondary ion spectroscopy we investigated nitrogen distribution in the Cr-N-coating on the Al-substrate (Fig. 6). Zero coordinate corresponded to the aluminum substrate surface.

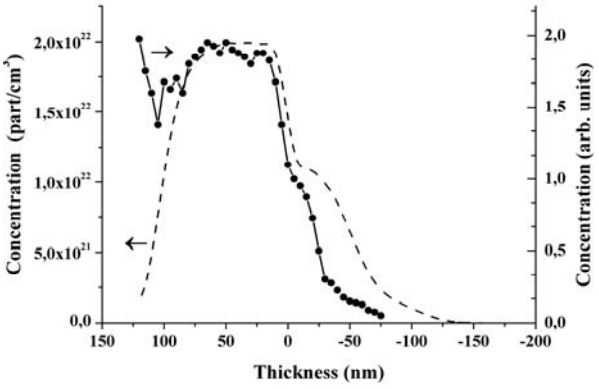

Fig. 6. Data on a change in relative nitrogen concentration in the aluminum substrate and Cr-N film obtained using the SIMP method (marker-drawn), a dashed curve shows computer simulation data. The left ordinate axis is related to the design data. The ion current density is 25 μA/cm², the deposition rate is 0.1 nm/s, and the temperature is 300 °C

Figure shows that nitrogen concentration in a film reached constant stationary value, because the film thickness exceeded the thickness of the transition zone. Our attention is focused on an abrupt increase in nitrogen concentration at the film-substrate boundary and the concentration curve bent for aluminum at a depth of 25 nm. This Figure also gives computation data shown by the dashed line. Computation results fit well experimental data and reproduce special features of a nitrogen concentration curve. At the same time the mismatch of the design and experimental data is observed near the film surface. A higher nitrogen content revealed on the surface confirms the results that were published earlier on the investigation of the phase composition of Cr-N composite at the initial stage of its formation in the ion irradiation environment [3]. The electron microscopy showed that chrome nitrides CrN and Cr_2N are formed at process temperatures exceeding 250 °C. The estimated nitrogen content in the film should not exceed 25%. Experimental investigations that were carried out testify that an increased value of nitrogen concentration at the growing film front can be related to the uptake of nitrogen from a residual atmosphere and formation of deposited metal nitrides within the chamber volume.

2. PECULIARITIES OF THE FILM STRUCTURE FORMATION AT THE INITIAL STAGE OF THE IBAD PROCESS

The results of computer simulation of a coating deposition process in the gas ion bombardment environment that are given in the next chapter show that the concentration of implanted ions and the amount of defects created by them change at different process stages. Therefore the conditions at which the coating structure is nucleated and formed will be different. This becomes especially topical for the deposition of coatings using the ion beam-assisted technology because the control over coating deposition processes at the initial stage defines in the long run the formation of the substrate-coating transition zone structure and a coating adhesion.

The previous papers that delved into the studies of the initial stage of coating formation [4, 5] studied mainly the influence produced by the bombardment with inert gas ions on the nucleation of a coating structure. It has been shown that the ion bombardment results in the promotion of the coalescence of grain nuclei and formation of coatings with an explicit texture.

While creating nitride coatings nitrogen ions should inevitably be used as bombarding particles since their presence must influence not only the structure of condensates but also their phase composition. The analysis of curves in Figs. 3 and 4 showed that the component composition and structure of films can continuously be changed until the thickness of 60 to 80 nm is reached. This happens due to the implantation of nitrogen ions and an increase in the amount of radiation defects created by them.

While studying the initial stages of the structure formation, for example, nitride coatings exposed to the ion bombardment attention should be paid to the nitrogen affinity to a definite material, i.e. to a value of Gibbs free energy of the given nitrides. The papers [6, 7] showed that the amount of nitrogen that can be adsorbed by the metal surface depends on the value of Gibbs free energy of appropriate nitrides.

In particular Fig. 7,a gives theoretical relationships of N/Me ratio taken from the paper [7] for the series of nitrides exposed to the bombardment with argon ions in

nitrogen environment as a function of their Gibbs energy. Fig. 7,b gives data taken from the paper [8], which show that using the same parameters for the irradiation of titanium whose nitride has low Gibbs energy with nitrogen ions its content in the material cardinally depends on nitrogen pressure.

The irradiation up to a maximum tested dose of 10^{17} ion/cm^2 at nitrogen pressure of $1\cdot10^{-4}$ Pa results in 90% nitrogen saturation and the pressure of $1\cdot10^{-3}$ Pa provides 100 percent saturation and irradiation dose-independent saturation occurs at $2\cdot10^{16}$ ion/cm^2. For comparison the diagram gives data for iron whose free energy of nitride formation is much higher than that of titanium, in particular 8.5 kcal/mole. It is seen that a change in nitrogen pressure by two and a half orders actually results in no change of its content in iron.

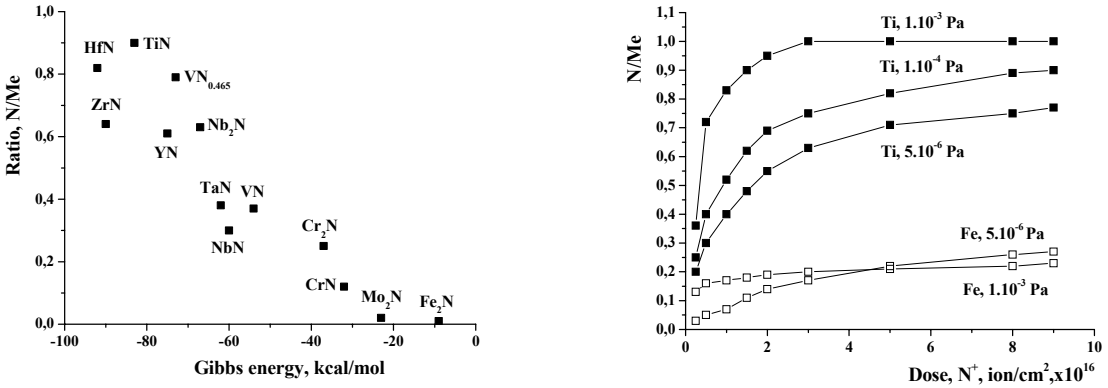

a *b*

Fig. 7. Relation between the saturation surface nitrogen-to-metal ratio and: a – Gibbs energy of nitride formation at 298 K for various metals bombarded with 8 keV Ar^+ ions at 4 μA·cm^{-2} in nitrogen at 10^{-3} Pa [7]; b – dose nitrogen ion irradiation (E=6 keV) at different nitrogen pressure [8]

We performed electron microscopy of initial stages of the formation of vanadium and chrome-nitride films that possess different Gibbs energy in conditions of ion-assisted deposition [9]. Figs. 8, 9 give distribution histograms of film grains whose effective thickness is in the range of 5 to 20 nm.

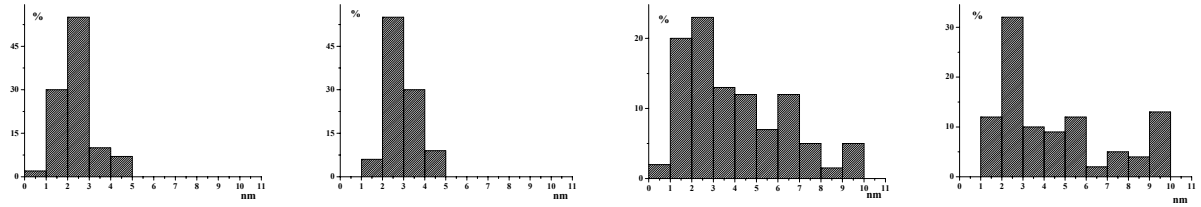

5 nm 10 nm 15 nm 20 nm

Fig. 8. Histograms of size distribution of grains in four CrN films [9]

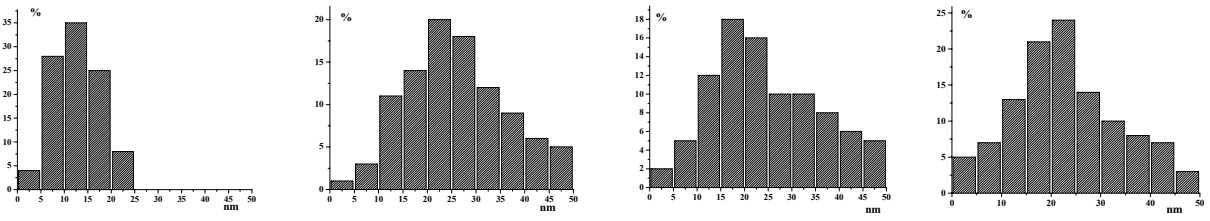

5 nm 10 nm 15 nm 20 nm

Fig. 9. Histograms of size distribution of grains in four VN films [9]

The analysis of histograms of CrN grain distribution for different deposition time showed that the material structure at the given stage corresponds to the grain nuclei system whose distribution function changes with an increase in the deposition time and irradiation dose. The first two films show uniform-sized distribution with sufficiently narrow peak for the size range of ≈ 2…3 nm, however starting from the third film the origination of nuclei of ≈ 5…8 nm is observed. This tendency is explicitly manifested in the fourth film.

It should be noted that an increase in the average size of nuclei occurs due to the appearance of the second peak in the region of large sizes, and not because of peak displacement on the distribution curve. The amount of small-size nuclei remains actually unchanged. This is indicative of the progress of coalescence process with simultaneous nucleation of

new grain population on vacant substrate sections. Vanadium grain size distribution curves have one maximum which shifts on the size scale from 15 to 25 nm as the film thickness is increased. Further deposition results in no shift of the given peak toward large sizes. In addition, an increase in the amount of small –size grains is observed, which occurs due to their origination on triple and quadruple grain junctions, not in the substrate plane. Due to the fact that the new grain population shades the space of intergranular junctions the formation process of a solid coating turns out to be incomplete. As a result the formed coating contains many pores of ~ 10 nm.

The diffraction analysis of chrome films showed that starting from the lowest thicknesses the formation of the crystalline structure of CrN occurs. Thereat, with an increase in the thickness of films their crystalline orientation is changed. The sequential orientation transition [211] → [211] + [100] → [100] is observed. A change in the structure of V films differs from that of Cr films. At low thicknesses a film consists of fully disoriented grains whose diffraction reflections form an annular electron-diffraction pattern. As the coating deposition time increases the texture formation in the direction (001) occurs. The film structure corresponds to the fcc phase of vanadium nitride VN_{1-x}. The attention is arrested by the fact that the vanadium nitride grain nuclei density does not exceed the value of $1.2 \cdot 10^{11}$ cm^{-2}, while for chrome nitride the nuclei density varied in the range of $6 \cdot 10^{11} \ldots 2 \cdot 10^{12}$ cm^{-2}.

Thus, we can state that in conditions of the irradiation with nitrogen ions during the chrome deposition a fine-crystalline dense structure is formed. The vanadium deposition in the same conditions results in the formation of a larger-grain messy structure. And finally, in spite of the fact that the estimated value of N^+/Cr,V ratio does not exceed 0.08 at the initial stage of coating formation (for thicknesses of 20 nm) the nitride phase is formed in both cases. The differences in formation processes of CrN_{1-x} and VN_{1-x} coatings can be explained within the framework of nitride formation thermodynamics. Fig. 7,a shows that for vanadium nitride the Gibbs energy is considerably lower in comparison with that of chrome nitride. Hence, nitrogen will react with vanadium more actively during the formation of nitride coatings by the ion-assisted deposition.

The deposition of vanadium and chrome occurs in conditions of continuous adsorption of nitrogen molecules by the substrate surface. The nitrogen dissociation energy is rather high and it reaches 205.8 kcal/mole, and therefore nitrogen fails to dissociate on the substrate at 200 °C. Its dissociation seems to be more feasible in ion-assisted process conditions. This mechanism can take place if specificity of the statement of IBAD experiments is taken into consideration. For this technology a vacuum space right before the substrate is in the effective area of bombarding ions. At such a configuration the probability of the dissociation of molecular nitrogen in the chamber volume is rather high. This may result in the formation of chemical compounds both in the chamber and on the substrate surface. It means that this method of coating deposition allows for the formation of compounds at the initial stage in two ways, in particular on the substrate due to the surface diffusion of metal and nitrogen atoms and due to the formation of nitride molecules in space, their deposition and diffusion.

A criterion of applicability of either mechanism for ion-assisted technology can be a degree of nitrogen affinity to metal. The fact that nitrogen reacts easier with vanadium in comparison with chrome allows us to assume that major portion of stable VN molecules is formed at the earliest stage of the process, i.e. during spatial interaction of dissociated vanadium and nitrogen molecules. On the contrary the formation of chrome nitride mainly occurs after the deposition of metal onto the substrate surface.

In the paper [9] we substantiated that vanadium nitride molecules have a longer lifetime while depositing on the substrate surface and display higher diffusion mobility in comparison with individual chrome and nitrogen atoms. Therefore, while forming a coating by combining clusters into stable nuclei, the distribution density of those nuclei should be lower than the density of structures formed due to the atom merging. In the case of chrome nitride the nuclei density is defined by the diffusion mobility both of chrome atoms and nitrogen atoms and by the time of their existence on the substrate. Each of these parameters will be lower than those for VN clusters that were formed prior to their appearance on the substrate. Due to this fact the chrome nitride structure should be more fine-grained than that of vanadium nitride as the experiment showed.

3. STRUCTURE AND PHASE CHARACTERISTICS OF "THICK" FILMS AND COATINGS

It was mentioned above that the reactive gas used for the IBAD technology enters a formed coating by two channels, in particular in the form of accelerated ions and adsorbed molecules. In spite of low pressure of a working gas in the vacuum chamber and taking into account relatively low deposition rates used for this method that range from -0.1 to 1.0 nm/s the amount of gas absorbed during the deposition can considerably exceed the number of deposited metal atoms. Therefore, the phase composition and coating structure depend directly on the amount and final state of gas present in the metal lattice, to be more exact to what extent specific material reacts with gas being used.

Use of the IBAD technology allowed for more detailed analysis of a Cr-N compound. In particular, Ensinger et al. [10] showed that coatings with different phase composition (Fig. 10) can be obtained by varying evaporation rate and ion current density. In order to form a stoichiometric CrN compound it is necessary to use low deposition rate of 0.1 to 0.3 nm/s and high ion current densities. However, all X-ray pictures show the reflection from the chrome lattice even at high densities.

In contrast to chrome transient metals of the fourth group, such as Ti, Hf, Zr have high affinity to reactive gases, therefore in conditions of ion-assisted deposition

it is possible to obtain nitrides that contain no metal component (Fig. 10,b) [11].

As it was mentioned above the ion bombardment during metal deposition contributes to an increase in the concentration of grain nucleation places and diffusion mobility both of individual atoms and Me-(N,C,O) compounds. This results in a change of the formation mechanism of grain nuclei. The grains become equiaxed and the content of gas impurities is decreased. The diffusion mobility of atoms is defined not so much by the substrate temperature as by ion current density. The nucleating structure is characterized by high grain density, small size (in nanorange) and narrow peak in the grain size distribution.

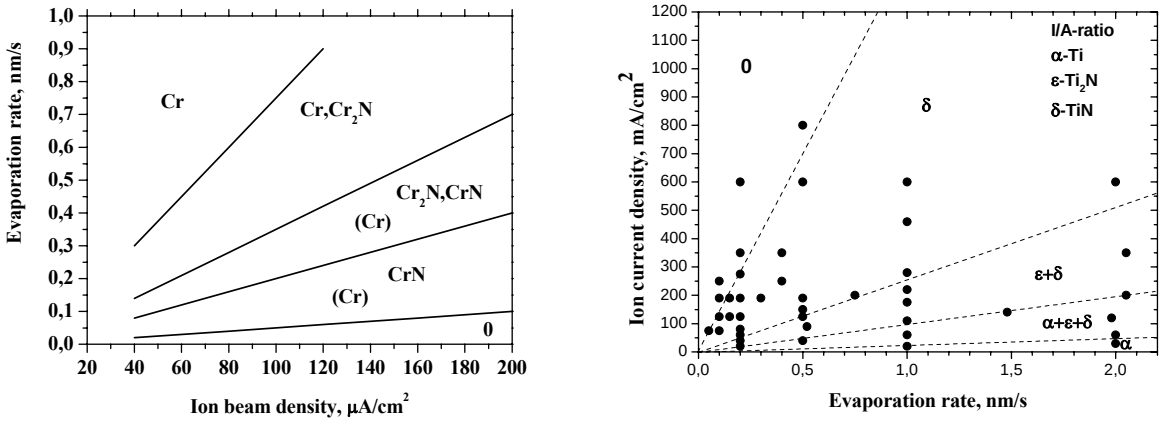

a *b*

Fig. 10. Regions of existence of different phases in the deposition rate/ion irradiation intensity diagram. a – Cr-N [10], b – Ti-N [11]. Ion energy – 30 keV

To stabilize the nanocrystalline structure and to improve consequently tribological characteristics the IBAD process is complemented with the evaporation or sputtering of the second metal, i.e. the three-component compounds are created [12]. A simultaneous deposition of two components requires the creation of appropriate conditions for the formation of nanocrystalline solid nitride phase surrounded by the second phase. In order to provide phase separation were selected metals that form no triple alloy Me_1Me_2N in their equilibrium state [13, 14]. The creation of nanocomposite structure is controlled by the process temperature and gas ion density. Nitrogen ions provide the formation of a solid nitride phase on the basis of one metal and a temperature provides diffusion of the second metal to the boundaries of nitride grains [14]. This configuration allows for the creation of composite structures with different phase ratio by varying metal percentage, substrate temperature, and energy density imparted by the ion beam. As a rule, such materials demonstrate the highest hardness and acceptable tribological characteristics when the size of their grains approaches 5 to 10 nm [12-14]. In such cases the intergranular space is filled very often with amorphous or crystalline boundary region.

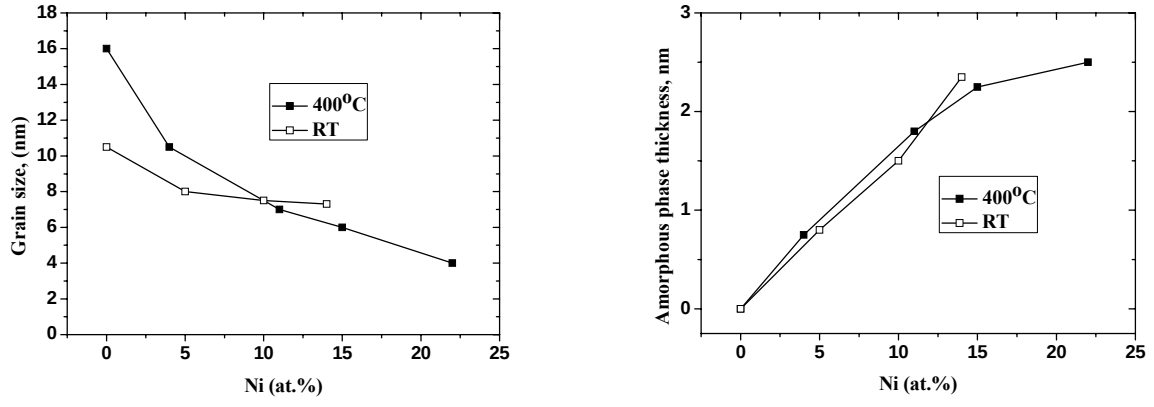

a *b*

Fig. 11. a – the grain size as a function of Ni content in the Ti-Ni-N coating. b – normalized average intergranular distance between TiN grains as a function of Ni content [14]

Fig. 11,a gives the relationships of grain sizes of the Ti-Ni-N film as a function of Ni content [14]. It is seen that in the absence of nickel the grain size is higher for the deposition at 400 °C. This means that the governing factor is the mobility of titanium and titanium nitride atoms. The addition of nickel results in its segregation at the nuclei boundaries of TiN grains and the blocking of their growth. As a result the grain size is decreased. The

radiation-assisted nickel diffusion and not temperature becomes the basic factor that defines the grain size. As the nickel content is increased actually the same increase in thickness of amorphous nickel layer between the grains occurs at room temperature and 400 °C (see Fig. 11,b).

4. TRIBOLOGICAL CHARACTERISTICS

It is believed that coatings with high tribological characteristics should meet three basic requirements, in particular the portion, which is contiguous with the article, should possess a good article adhesion and the external portion of a coating should sustain loadings to which the article is exposed during the operation and an interim region must damp these loadings. In the classic case to solve this problem it is necessary to apply a three-layer coating in which each layer fulfills the required function. Naturally, the main parameter that defines the quality of transition zones between the layers will be a temperature of a coating deposition process. In the IBAD technology the function of temperature is fulfilled by the flow density of gas ions and their energies.

For example, W. Ensinger et al. [15] analyzed the quality of TiN coatings applied onto AlSI 52100 and aluminum alloy $AlCuMg_2$ using the IBAD method. It has been shown that structural and tribological characteristics of a coating are mainly defined by the ion beam energy and density. For the range of mean and high energies of 10 to 20 keV the coatings that were obtained using the IBAD method demonstrate higher tribological characteristics, in particular adhesion, wear-resistance and hardness in comparison with those that were deposited using traditional PVD methods.

4.1. MICROHARDNESS

It is known that the hardness of polycrystalline structures is defined by their microstructure. In order to have an increased hardness the structure should be able to suppress the formation and motion of dislocations and microcracks. This problem can be solved in many ways, in particular grain crushing, cold deformation, alloying and so on. However, these methods are not applicable to the case of nanocrystalline objects since the alloying ions leave the grain volume and segregate on its boundaries and the dislocations are not formed at all. Therefore, the microhardness of films obtained in ion bombardment conditions is defined by process parameters and a possibility to alloy the grain boundaries of a single-phase material by the second phase.

The papers [16-19] studied the influence produced by the ion energy and ion current density on microhardness of Cr-N coatings (Fig. 12). Lower values of microhardness were obtained in the paper [17] that used high densities of ion streams of 100 to 120 $\mu A/cm^2$; as a result the coating structure was a mixture of Cr + Cr_2N. The transition to lower intensities of ion current [18] results in the formation of CrN phase and an increase in microhardness. The increase was insignificant, possibly due to the large size of a coating grain, i.e. 200 nm. The papers [16, 19] used higher energies that defined an increase in microhardness up to 18…30 GPa. The highest increase was demonstrated by coatings with the smallest grain size of 5 to 8 nm [16].

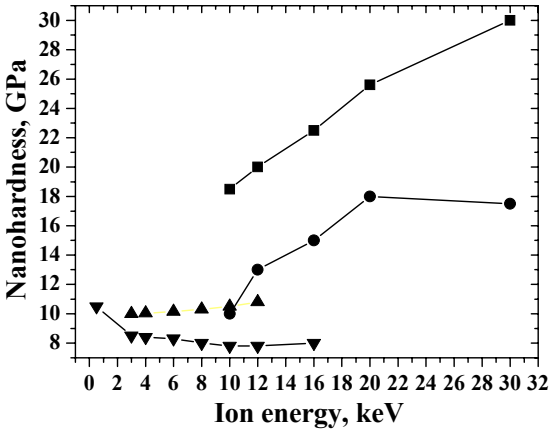

Fig. 12. Dependences of microhardness of CrN coatings on the energy of bombardment ions.
● – [16]; ▲ – [17]; ▼ – [19]; ■ – [18]

The data given above with regard to the influence produced by experimental parameters of the IBAD-process on microhardness of a Cr-N coating show that not only the phase composition influences this value but also the grain size. It was noted time and again that the Hall-Patch formula cannot be applied to nanocrystalline structures with the size grain of < 10 to 20 nm (for example 20, 21) and the microhardness value can exceed the estimated value by a factor of 4 to 5. Today many models are available that could explain the observed effect. It is known, for example, that availability of a large amount of low-angle boundaries in a fine-grained structure creates conditions for the appearance of a stressed state in films [22]. As a rule, metal films deposited without ion stimulation experience tensile internal stresses that crave for the compensation of porosity that occurs at grain boundaries. The deposition of chrome in the ion-bombardment conditions cardinally changes the situation. As a rule an increase in the amount of energy introduced by the ion beam results in the change of the stress sign replacing tensile stresses by compressive ones [23-25].

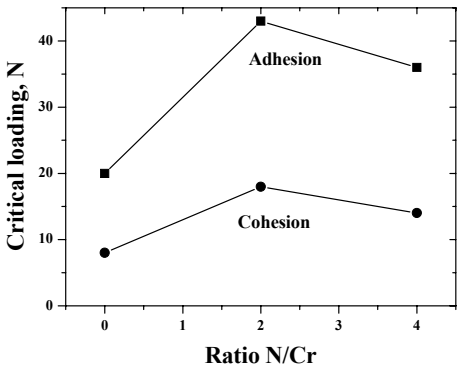

Fig. 13. Dependence of a critical load of CrN coating separation on N/Cr ratio value [26]

Fig. 13 shows the relationships of stress values in Cr-N coatings as a function of N/Cr ratio [26]. Such a trend of curves correlates with an increase in the CrN phase and decrease in the grain size revealed in the

same work. That is, an increase in microhardness of CrN films with a decrease in the grain size is explained by an increase in compressive stresses. The grain value is just a parameter convenient for the comparison of different data [27].

4.2. ADHESION

The adhesion characteristics of coatings applied using ion bombardment technologies are defined by many factors, in particular careful preparation of the substrate surface, substrate-coating mixing zone depth, the formation efficiency of chemical compounds in the transition zone and also by the absence of both increased stresses and segregation of gas mixtures in this zone. The ion bombardment during the deposition ambiguously affects each factor mentioned above.

The papers [26, 28] studied the influence of the ion energy on the adhesion value of the Cr-N coating. The authors did not manage to establish direct interrelation between the energy of nitrogen ions and the adhesion value [28]. On the contrary, the increase in energy from 20 to 40 keV resulted in a decreased adhesion.

For additional improvement of adhesion characteristics of coatings we used the method of stimulation of mutual substrate-coating mixing through the preliminary implantation of nitrogen ions into the substrate with energy of 30 keV to reach doses at which the substrate surface layer is saturated with nitrogen up to the concentration of Me/N = 1. The process temperature is not high and reaches 200 °C. Then the irradiation is continued and the metal is deposited using the electron -beam evaporation technique, i.e. a duplex IBAD process [29]. The coating thickness is 130 nm. Fig. 14 gives Cr and Nb distribution curves depending on the depth for the case of ordinary IBAD process (a) and for the case of duplex treatment, i.e. implantation +IBAD process (b).

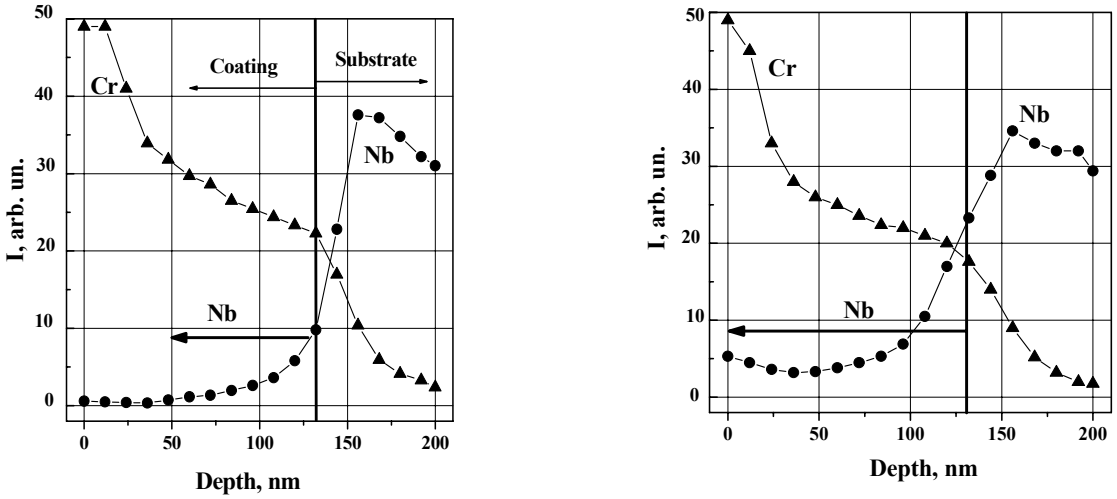

a *b*

Fig. 14. Cr and Nb distribution in a coating-substrate combination for the ordinary IBAD process (a) and for the duplex process, implantation $3.5 \cdot 10^{17}$ cm^{-2} + IBAD (b) [29]

It is seen that in spite of relatively low temperature of the experiment, the high flaw level peculiar for the IBAD technology contributes to the intensive progress of diffusion processes and formation of rather broad mixing zone. A preliminary ion bombardment stimulates this process even more.

4.3. FRICTION COEFFICIENT AND WEAR

Comprehensive study of the friction coefficient and wear-resistance of CrN and TiN coatigs applied onto AlSI H13 steel was done in the paper [30]. It has been shown that the friction coefficient of CrN coatings applied on corundum at a relative humidity (RH) of 50 and 85% was about 0.3, slightly higher than that of TiN coatings. At RH < 10% , it is a little bit higher but still has a low value before complete wear of CrN coatings, whereas TiN coatings exhibit the high coefficient of friction of about 0.8. In addition, a volumetric loss of CrN coatings during their friction is smaller in comparison with that of TiN coatings, especially at low RH.

The influence of Cr/N ratio and the energy of nitrogen ions on the wear of CrN coating applied onto AISI 52100 steel were studied in the paper [16]. It has been shown that the fraction of Cr_2N phase is increased in the coating with an increase in Cr/N ratio and the wear is also cardinally increased (Fig. 15). A three-fold increase in the ion energy produces actually no impact on the wear-resistance.

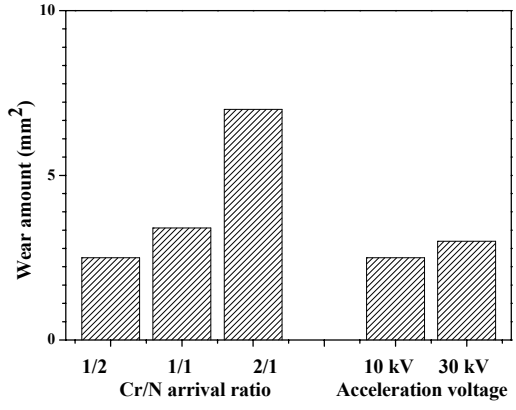

Fig. 15. Wear of Cr-N coating after 200 test cycles as a function of Cr/N arrival ratio and ion energy [16]

Studying the influence produced by the basic parameters of the IBAD process (the ion energy and beam current density) on tribological characteristics of CrN coating showed that the friction coefficient slightly depends on both parameters [18]. The wear-resistance is significantly increased in coated steel. The range of currents' densities embracing 8 to 32 μA/cm^2 and energies of 4 to 12 keV has been studied. The most optimal are energy values of 12 keV and minimal values of current density are 8 μA/cm^2.

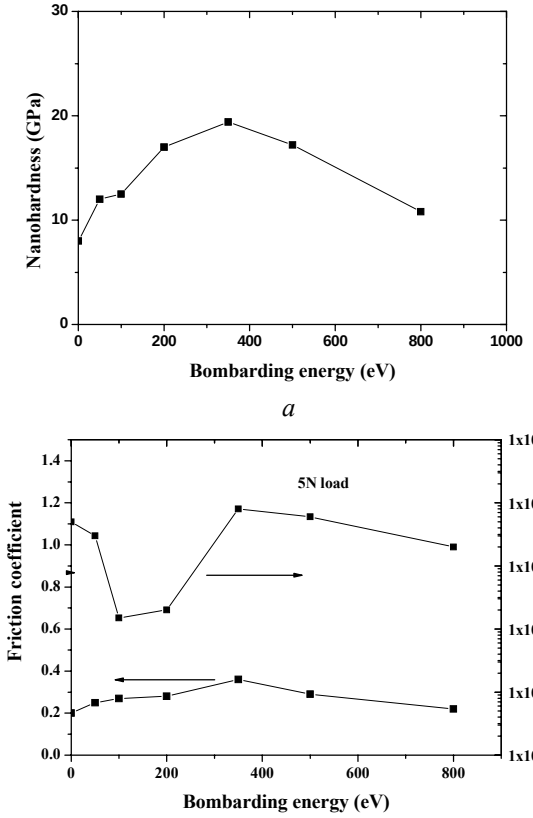

Fig. 16. Nanohardness (a), friction coefficient and wear (b) of TiBN synthesized at different bombardment energy [31]

The deposition of a three-component TiBN coating in conditions of low-energy radiation [31] showed that the change in the ion energy in the range of 0 to 800 eV cardinally changes hardness, friction coefficient and wear-resistance (Fig. 16). It is seen that the most acceptable values are reached at different energy values: a maximum hardness is reached at 400 eV and a minimum wear and friction coefficients are observed at 150 eV. The structure of TiBN composite consists of nanocrystals TiB_2 and TiN surrounded by a soft h-BN phase. At such a configuration the best tribological characteristics are obtained at optimum mixing of nanograins in the soft phase. An increase in hardness with an energy increase can be explained by that the rise in the ion energy up to 400 eV and higher results in the preferred sputtering of lighter coating components B and N. As a result the share of a harder component of TiN is increased and this contributes to an increase in hardness of TiN coatings at high energies. At lower energies a softer h-BN phase defines tribological properties to a large extent.

CONCLUSIONS

The research done in the field of nanostructured material science over the last few years showed that materials with ultrafine grain have great prospects for the heavy-duty operation. The production of such materials is impossible using equilibrium technologies, Therefore the interest in nanocrystalline materials stimulated the development of technologies based on nonequilibrium processes. In particular ion assisted deposition technologies are widely used for the formation of thin-film structures. High operating performances of the obtained coatings are defined by that the ion bombardment in combination with the deposition of atomic-&- molecular flows give an opportunity to design their structure on the atomic level. The intensive irradiation with heavy charged particles in combination with the deposition of overheated metal vapors onto the "cold" substrate creates conditions for the formation of structures with the grain size less than 10 nm. By varying such parameters as ion current density, ion energy, nitrogen/boron/carbon/oxygen content and metal component concentration we can create structures whose tribological characteristics can vary in wide ranges.

An additional advantage of the ion beam-assisted technology is that it can be used for the deposition of protective coatings onto the material with low melting temperature. Also is very important that the evaporation of metals with different affinity to active gases allows for the purposeful design of multicomponent structures that include both metal nanocrystalline grains and amorphous/ crystalline nitride (boride and carbide) phases.

REFERENCES

1. J.F. Ziegler. www.srim.org.

2. A. Guglya, I. Marchenko, I. Neklyudov. Production of Cr-N films by ion beam-assisted deposition technology: experiment and computer simulation // *Surf. Coat. Technol.* 2003, v. 163-164, p. 286-292.

3. A. Goncharov, A. Guglya, I. Marchenko, I. Neklyudov. Investigation of nitrogen distribution in samples produced by ion-induced deposition of Cr films on aluminum under nitrogen ions bombardment // *Vacuum*. 2004, v. 76, p. 299-302.

4. M. Marinov. Effect of ion bombardment on the initial stages of thin film growth // *Thin Solid Films*. 1977, v. 46, p. 267-274.

5. J. Arnault, J. Delafond, C. Templier, et al. First stages study of high energy ion beam assisted deposition // *Nucl.Instr. & Meth.Phys. Res.* 1993, v. B80/81, p. 1384-1387.

6. Y. Baba, T. Sasaki. Nitride formation at metal surfaces by Ar^+ ion bombardment in nitrogen atmosphere // *Mat. Sci. & Eng.* 1989, v. A 115, p. 203-207.

7. I. Barin, O. Knacke. *Thermodynamical properties of inorganic substances.* Springer: Berlin, 1973, 126 p.

8. I. Takano, S. Isobe, T. Sasaki, Y. Baba. Nitrogenation of various transition metals by N^{2+}-ion

implantation // *Applied Surface Science,* 1989, v. 37, p. 25-29.

9. A. Guglya. Electrofisicheskie I strukturno-fasovye charakteristiki tonkoplenochhyh kompositov Cr-N i V-N // *Vestnik Kharkovskogo universiteta.* 2005, v. 664, №2(27), p.73-78.

10. W. Ensinger, M. Kiuchi. The formation of chromium/nitrogen phases by nitrogen ion implantation during chromium deposition as a function of ion-to-atom arrival ratio // *Surf. & Coat. Tech.* 1997, v. 94-95, p. 433-436.

11. W. Ensinger, B. Rauschenbach. Microstructural investigation on titanium nitride films formed by medium energy ion beam assisted deposition // *Nucl. Instr. & Meth. in Phys. Res.* 1993, v. B80/81, p. 1409-1414.

12. A. Akbari, J.P. Riviere, C. Templier, E. Le Bourhis. Hardness and residual stresses in TiN-Ni nanocomposite coatings deposited by reactive dual beam sputtering // *Rev. Adv. Mater. Sci.* 2007, v. 15, p. 111-117.

13. C. Zhang, J. Luo, W. Li, D. Chen. Mechanical properties of nanocomposite TiN/Si_3N_4 films synthesized by ion beam assisted deposition (IBAD) // *J. Tribol.* 2003, v. 125, №2, p. 445-447.

14. A. Akbari, J. Riviere, C. Templier, E. Bourhis. Structural and mechanical properties of IBAD deposited nanocomposite Ti-Ni-N // *Surf. & Coat. Tech.* 2006, v. 200, p. 6298-6302.

15. W. Ensinger, A. Schröer, G. Wolf. A comparison of IBAD films for wear and corrosion protection with other PVD coatings // *Nucl. Instr. & Methods in Phys. Res.* 1993, v. B80/81, p. 445-454.

16. A. Vanzha, A. Guglya. Mikrotverdoct i adgezia Cr-N i V-N pokrytiy poluchenyh s ispolzovaniem iono-stimulirovanoy tehnologii // *Metalophysika i noveyshie tehnologii.* 2007, v. 29, N 9, p. 1185-1199 (in Russian).

17. P. Engel, G. Schwarz, G. Wolf. Corrosion and mechanical studies of chromium nitride films prepared by ion-beam-assisted deposition // *Surf. & Coat. Tech.* 1998, v. 98, p. 1002-1007.

18. Y. Fu, X. Zhu, B. Tang, et al. Development and characterization of CrN films by ion beam enhanced deposition for improved wear resistance // *Wear.* 1998, v. 217, p. 159-64.

19. K. Sugiyama, K. Hayashi, J. Sasaki, et al. Basic characteristics of chromium nitride films by dynamic ion beam mixing // *Nucl. Instr.&Meth. in Phys. Res.* 1993, v. B80/81, p. 1376-82.

20. K. Lu. Nanocrystalline metals crystallized from amorphous solids: nanocrystallization, structure and properties // *Mater. Sci. Eng.* 1996, v. R16, p. 161-221.

21. R. Andrievski. State-of-the-art and perspectives in the field of particulate nanostructured materials // *J. Mater. Sci. Technol.* 1998, v. 4, p. 97-103.

22. L. Palatnik, M. Fuks, V. Kosevich. *Mekhanism obpasovaniya i substruktura kondensirovanyh plenok.* Moscow: "Nauka", 1972, 183 p. (in Russian).

23. P. Mayrhofer, G. Tischler, C. Mitterer. Micro-structure and mechanical/thermal properties of Cr-N coatings deposited by reactive unbalance magnetron sputtering // *Surf. & Coat. Tech.* 2001, v. 142-144, p. 78-84.

24. M. Oden, J. Almer, G. Hakansson, M. Olsson. Microstructure-property relationships in art-evaporated Cr-N coatings // *Thin Solid Films*. 2000, v. 377-378, p. 407-12.

25. A. Ehrlich, M. Kühn, F. Richter, W. Hoyer. Complex characteristics of vacuum arc-deposited chromium nitride films // *Surf. & Coat. Tech*. 1995, v. 76-77, p. 280-286.

26. J. Demaree, C. Fountzoulas, J. Hirvonen. Chromium nitride coatings produced by ion beam assisted deposition // *Surf. & Coat. Tech*. 1996, v. 86-87, p. 309-315.

27. C. Chuang, C. Chao, R. Chang, K. Chu. Effect of internal stresses on the mechanical properties of deposited thin film // *J. Mat. Proc. Tech.* 2008, v. 201, p. 770-774.

28. L. Tian, B. Tang, D. Liu, et al. Interfacial reactions during IBAD and their effects on the adhesion of Cr-N coatings on steel // *Surf. & Coat. Tech.* 2005, v. 191, p. 149-54.

29. A. Guglya, I. Neklyudov, V. Shkuropatenko, et al. Composition compound of Cr-N coating deposited on the aluminium preliminary irradiated with nitrogen ions // *Problems of Atomic Science and Technology.* 2005, v. 86, N 3, p. 171-175.

30. H. Chen, P. Wu, C. Quaeyhaegens, et al. Comparison of fretting wear of Cr-rich CrN and TiN coatings in air of different relative humidities // *Wear*. 2002, v. 253, issue 5-6, p. 527-532.

31. J. He, S. Miyake, Y. Setsuhara, et al. Improved anti-wear performance of nanostructured titanium boron nitride coatings // *Wear.* 2001, v. 249, p. 498-502.

Статья поступила в редакцию 29.01.2014 г.

ИОННО-СТИМУЛИРОВАННАЯ ТЕХНОЛОГИЯ – МЕТОД СОЗДАНИЯ НАНОКРИСТАЛЛИЧЕСКИХ ПОКРЫТИЙ

Обзор

А.Г. Гугля, И.Г. Марченко

Дается описание структуры, фазового состава и механических характеристик нанокристаллических покрытий, полученных с использованием технологии ионно-стимулированного осаждения (IBAD method). Приводятся результаты компьютерного моделирования IBAD процесса для различных энергий бомбардирующих ионов и различных соотношений между скоростью осаждения покрытий и плотностью ионных потоков. Представлены данные электронно-микроскопических исследований начальной стадии формирования нанокристаллических структур (толщиной 5 нм и больше). И наконец, продемонстрированы влияние энергии ионов и плотности ионных потоков на формирование нанокристаллических структур и их корреляция с трибологическими свойствами покрытий.

ІОННО-СТИМУЛЬОВАНА ТЕХНОЛОГІЯ – МЕТОД СТВОРЕННЯ НАНОКРИСТАЛІЧНИХ ПОКРИТТІВ

Огляд

О.Г. Гугля, І.Г. Марченко

Приводиться опис структури, фазового складу та механічних характеристик нанокристалічних покриттів, які здобуваються з використанням технології іонно-стимульованого осадження (IBAD method). Приводяться результати комп'ютерного моделювання IBAD процесу для різних енергій бомбардуючих іонів та різних співвідношень між швидкостями осадження покриттів та щільністю іонних потоків. Представлені також дані електронно-мікроскопічних досліджень початкової стадії формування нанокристалічних структур (товщиною 5 нм и вище). В останньому розділі продемонстровано вплив енергії іонів та щільності іонних потоків на формування нанокристалічних структур та їх кореляція з трибологічними властивостями покриттів.